2018 *Macromolecules* **2010**, *43*, 2018–2027
DOI: 10.1021/ma902366c

Macromolecules
ARTICLE

Path-Dependent Morphology and Relaxation Kinetics of Highly Amphiphilic Diblock Copolymer Micelles in Ionic Liquids

Luciana Meli,[†] Jessica M. Santiago,[†] and Timothy P. Lodge*[,†,‡]

[†]*Department of Chemistry and* [‡]*Department of Chemical Engineering and Materials Science, University of Minnesota, Minneapolis, Minnesota 55455*

Received October 23, 2009; Revised Manuscript Received January 5, 2010

ABSTRACT: The role of kinetics in the formation and relaxation of highly amphiphilic diblock copolymer micelles in ionic liquids is analyzed. In particular, we studied the morphology of poly(butadiene)−poly(ethylene oxide) (PB−PEO) block copolymer micelles dispersed in 1-ethyl-3-methylimidazolium bis(trifluoromethyl sulfonyl)imide [EMI][TFSI] and prepared via two methodologies: direct dissolution (DD) and cosolvent-aided dissolution (CS). Dynamic light scattering (DLS) measurements reveal that the former procedure leads to large and polydisperse aggregates that relax upon annealing at high temperatures into smaller and narrowly distributed, steady-state spherical micelles, while the latter protocol results in smaller, monodisperse micelles that retain their size upon prolonged thermal treatment. Remarkably, the CS micelles are only half the size of the annealed DD micelles. The development of distinct, steady-state micellar distributions through the two preparation protocols is consistently observed when changing the selectivity of the solvent (by changing the cation to 1-butyl-3-methylimidazolium) or by substituting the core-forming PB block for a polystyrene chain. Two different distributions were also observed when changing the solubility of the copolymer through variation of the corona block length. A better understanding of the underlying mechanism of DD-micelle relaxation is obtained by measuring the temperature-dependent relaxation of the micelles using DLS. In all cases the relaxation is well described by an Avrami-type relaxation function with exponent $n = 2$. The resulting relaxation times decrease with increasing copolymer concentration, suggesting that fusion/fission is the main mechanism of DD-micelle relaxation, and with annealing temperature. The results are in agreement with complementary small-angle neutron scattering experiments that reveal no single chain exchange between steady-state PB−PEO micelles in the imidazolium-based ionic liquid, up to at least 200 °C.

Introduction

The self-assembling capabilities of block copolymers in selective solvents have been widely exploited for the production of micellar nanostructures in various applications from drug delivery[1,2] to dispersion polymerization, phase transfer,[3] and catalysis.[4] The versatility of these systems stems from the tunable nature of the shape, size, properties, and characteristic time scales of the aggregates, which are in turn controlled by the virtually unlimited combinations of block chemical structure, chain length, copolymer architecture, and solution conditions. The wealth of structures that can be prepared is further enriched by metastability, particularly with highly amphiphilic block copolymer chains. Kinetic entrapment of these nonergodic block copolymer aggregates is a result of the slow chain exchange between micelles, resulting from the extremely low critical micellar concentration (cmc) typical of these solutions.[5−7] The ability to predict kinetic pathways of micelle formation could provide access to a wide spectrum of potentially useful nanoparticles[8] and serve as simple models to better understand the self-assembly processes in more complex biological systems.[6] Moreover, since many of the aforementioned applications rely on the use of micelles as vessels that carry a variety of payloads, an understanding of the exchange kinetics of micelles and the overall control of aggregate lifetime can be crucial for the timely release of the different species.[9]

The first theoretical description of the relaxation dynamics in polymeric micelles was performed by Halperin and Alexander,[10] following the Aniansson−Wall mechanism originally proposed for surfactant micelles.[11,12] The basic assumption is that the exchange kinetics of block copolymer micelles is dominated by the stepwise insertion and expulsion of single chains. Multichain processes, particularly micelle fusion/fission, were found to be energetically unfavorable near equilibrium conditions and when the distribution of micellar sizes was sufficiently narrow. The relaxation behavior was shown to be characterized by two relaxation processes, where the faster relaxation of unimer exchange was predicted to have a single-exponential form. Since then, other theoretical treatments of the kinetics of micelle evolution involving large deviations from equilibrium, including the process of micellization itself, have arisen.[13−15] The work by Dormidontova[13] suggests that fusion of micelles can be the dominant mechanism of aggregate growth during the early stages of micellization, whereas unimer insertion gradually becomes predominant as equilibrium is approached. In contrast, Semenov and co-workers[15] used a theoretical model based on the high activation energies of submicellar species and argued that insertion/expulsion is the only energetically favorable mechanism for micelle formation and equilibration. The analysis also suggests that systems far from equilibrium are likely to evolve by a continuous spectrum of relaxation times.

Some experimental studies have shown that the relaxation of block copolymer aggregates can be satisfactorily fit by double-exponential functions, regardless of whether the perturbation applied leads to micellization/dissolution[16−18] or only to small changes in the equilibrium properties of the micelles,[19−22] such as

*Author for correspondence: lodge@chem.umn.edu.

those obtained from temperature jumps. The signals obtained have also been taken to represent a continuous spectrum of relaxation times.[17,23] More detailed time-resolved small-angle neutron scattering (TR-SANS) measurements of chain exchange have found approximately logarithmic time decays,[24−27] which have recently been quantitatively described by a single activated process with a hypersensitivity to core block polydispersity.[27]

It is important to emphasize that in most cases the kinetics of block copolymer micelle equilibration proceed over time scales that are substantially longer (seconds−days) than those characteristic of surfactant micelles[28] (microseconds−milliseconds) and are usually very sensitive to the quality of the solvent. This is the reason why in many instances the dynamics of the polymeric micelles have to be adjusted by addition of a cosolvent that lowers the incompatibility between the core block and the solvent.[9,17,24,29,30] This approach, however, is also likely to lead to some degree of swelling of the micellar core by the compatible solvent. A more direct approach is to control the micellar dynamics by variations in temperature. In practice, this strategy is not always applicable since most organic solvents and water possess a relatively high vapor pressure that often restricts the window of temperatures that can be accessed. In a recent report,[31] we overcame this limitation by the use of an ionic liquid as the solvent medium. Ionic liquids are molten salts with a host of attractive properties such as low melting points, negligible volatility, tunable solubility, and high thermostability.[32−35] In the past few years, research groups have begun to study the micellization of block copolymers in ionic liquids.[36−39] For the purpose of this work, the advantage of using ionic liquids to induce copolymer aggregation is that it allows us to control micellar dynamics over a wide range of temperatures and times scales.

We demonstrated[31] the strong path dependence of micellar structures formed by a particular poly(butadiene)−poly(ethylene oxide) block copolymer in the ionic liquid 1-ethyl-3-methylimidazolium bis(trifluoromethylsulfonyl)imide, [EMI][TFSI], by using three different preparation procedures: direct dissolution (DD), cosolvent dissolution (CS), and thin film dissolution (TF). Dynamic light scattering (DLS) measurements revealed that DD and TF methodologies initially led to large and polydisperse aggregates that eventually evolved into a steady-state morphology of monodisperse, spherical micelles upon thermal treatment at high temperatures. In contrast, the CS procedure yielded smaller spherical micelles that remain unchanged upon extended thermal annealing. Remarkably, these CS micelles were only half the size of the annealed DD and TF micelles. Thus, at least one of the steady-state micelle populations (CS or DD/TF) remains far from equilibrium.

In this work, we expand on our understanding of the influence of the preparation procedure on micelle morphology by making systematic variations to the selectivity of the solvent through changes in the chemistries of the ionic liquid cation and of the core block as well as by changes in solubility of the copolymer through modification of the corona block length. We also explore the dynamics of DD micelle relaxation over a broad range of temperatures and concentrations using dynamic light scattering and correlate these results with supplementary measurements of the chain exchange kinetics between steady-state micelles using small-angle neutron scattering (SANS). The data are discussed in terms of the possible mechanisms of aggregate formation and relaxation.

Experimental Section

Materials and Solutions. The molecular characteristics of the polymers used in this study are included in Table 1. The three poly(butadiene)-*b*-poly(ethylene oxide) (PB−PEO) block copolymers were synthesized by Sangwoo Lee via a two-step anionic polymerization[40] and possess the same PB block length, but vary in the length of the PEO chain. They are designated BO(8−7), BO(8−15), and BO(8−20), where the numbers in parentheses indicate the number-average molecular weight of each block in kDa. A polystyrene-*b*-poly(ethylene oxide) block copolymer was also previously prepared by sequential anionic polymerization by Huiming Mao and will be referred to as SO(11−10).[41]

Table 1. Molecular Characteristics of the Diblock Copolymers

sample code[a]	M_n[b] (kDa)	M_{PEO} (kDa)	f_{PEO}[c]	PDI[d]
BO(8−7)	14	6.5	0.39	1.04
BO(8−15)	23	15	0.60	1.05
BO(8−20)	28	20	0.66	1.02
dBO(7−28)	35	28	0.74	1.06
SO(11−10)	21	10	0.45	1.04

[a] The molecular weights of the hydroxylated homopolymers (PB−OH, dPB−OH, or PS−OH) were determined from SEC measurements. The PB block microstructure reflects 90% 1,2-addition. [b] Number-average molecular weight obtained from the weight fraction of PEO in the diblock copolymers using ^{1}H NMR and from the molecular weight of the macroinitiator. [c] Volume fraction from ^{1}H NMR using the following amorphous densities: $\rho_{PB} = 0.87$ g/cm^3, $\rho_{PEO} = 1.13$ g/cm^3, and $\rho_{PS} = 1.05$ g/cm^3. [d] Polydispersity index determined using SEC.

In addition, a BO diblock copolymer with a deuterated PB block (dPB) was prepared specifically for use in the SANS experiments described below by employing a fully deuterated butadiene monomer (98 atom % D, Polymer Source, Inc.) in the two-step anionic polymerization. The molecular weight and PEO volume fraction of this diblock copolymer, dBO(7−28), are an approximate match for BO(8−20). The molecular weight, polydispersity, and composition of all the copolymers were determined by size exclusion chromatography (SEC) in conjunction with ^{1}H NMR spectroscopy.

The ionic liquid [EMI][TFSI] was prepared by anion exchange of equimolar amounts of 1-ethyl-3-methylimidazolium bromide [EMI][Br] (IoLiTec) and lithium bis(trifluoromethylsulfonyl)imide (IoLiTec) in distilled water at 70 °C for 24 h. The aqueous phase was subsequently removed, and the ionic liquid was washed repeatedly with distilled water. The ionic liquid was further purified by passing it through an alumina column using dichloromethane as a solvent. After purification, the dichloromethane was removed by blowing nitrogen at room temperature, and then the ionic liquid was dried under vacuum (< 50 mTorr) at 70 °C for 60 h. The same general scheme was used to prepare [BMI][TFSI], wherein the bromide salt, [EMI][Br], is replaced by 1-butyl-3-methylimidazolium bromide, [BMI][Br].

Two protocols were utilized for the preparation of the micellar solutions, i.e., direct dissolution (DD) and cosolvent-aided dissolution (CS). In the DD method, the ionic liquid and the polymer were mixed gravimetrically to achieve a concentration of 0.5 wt % and then stirred at 70 °C for 40 h. In the CS method, mixing of weighed amounts of polymer and ionic liquid was followed by addition of dichloromethane, a common solvent for both blocks, to a 1:1 w/w ionic liquid-to-dichloromethane ratio. After complete dissolution of the polymer, the cosolvent was gradually removed by stirring the solution under a nitrogen purge for ~12 h to induce aggregation of the insoluble block (PB or PS, depending on the copolymer).[37,42] The solution was then placed in a vacuum oven (< 50 mTorr) at 50 °C for 40 h to allow removal of residual dichloromethane.

A similar procedure was used to estimate the dichloromethane concentration at which micelle formation occurs for the BO(8−15) copolymer during the CS protocol. In this case, however, the polymer was initially dissolved in a 1:2 w/w [EMI][TFSI]-to-dichloromethane mixture, and DLS measurements were taken at regular concentration intervals during the slow evaporation process until a concentration of 1 wt % of polymer in pure [EMI][TFSI] was achieved.

A concentration series of 0.5, 0.25, 0.1, and 0.05 wt % was obtained by dilution of a 1 wt % BO(8−7)/[EMI][TFSI] micellar solution prepared using the DD protocol.

Solutions containing 1 wt % of BO(8−20) or of its deuterated analogue, dBO(7−28), in [EMI][TFSI] were prepared through both CS and DD protocols for SANS measurements. Postmixed samples were made by simply mixing the deuterated and protonated copolymer solutions (prepared using the same protocol) in a 1:1 ratio immediately before scattering measurements were taken. Additionally, a randomized blend of the copolymer pair was obtained by mixing solutions of the two copolymers in dichloromethane, followed by drying and annealing in a vacuum oven at 50 °C for 40 h. Premixed samples of the blended copolymers were then made by the CS and the DD procedures as explained above to yield 1 wt % solutions of the polymers in the ionic liquid.

Dynamic Light Scattering. Scattering measurements were performed on a home-built setup equipped with a Brookhaven BI-DS photomultiplier mounted onto an adjustable goniometer, a Lexel Ar^+ laser operating at 488 nm, and a Brookhaven BI-9000 correlator. Temperatures were controlled with an index-matching silicone oil bath to within ±0.2 °C. Samples were prepared by filtering the solutions through 0.45 μm GHP syringe filters into dust-free glass tubes with an inner diameter of 0.51 cm. The tubes were subsequently sealed in an argon atmosphere to prevent polymer degradation and absorption of moisture. In a typical thermal relaxation experiment, the tube was placed in the oil bath only after the desired temperature (120−170 °C) had been stabilized for at least 20 min. The intensity correlation function, $g_2(t)$, was then measured at a fixed 90° scattering angle and varying time intervals. The accumulation time for measuring $g_2(t)$ ranged from 90 to 240 s. Before and after every thermal relaxation experiment, scattering measurements were taken at 25 °C and five different scattering angles between 40° and 120° to corroborate the initial and final micelle size.

The measured $g_2(t)$ were then transformed to the electric field autocorrelation functions by using the Siegert relation,[43] $g_2(t) - 1 = g_1^2(t)$. The resulting functions were fit to the cumulant expansion (eq 1) using a nonlinear least-squares fitting method to evaluate the average decay rate, $\bar{\Gamma}$, and the variance, $\mu_2/\bar{\Gamma}^2$.

$$g_1(t) = A\exp(-\bar{\Gamma}t)\left(1 + \frac{\mu_2}{2!}t^2 + \ldots\right) \tag{1}$$

The mutual diffusion coefficients, D_m, were calculated using $D_m = \bar{\Gamma}/q^2$, where q is the scattering vector defined as $q = (4\pi n/\lambda_0)\sin(\theta/2)$, n is the refractive index of the solvent, λ_0 is the wavelength of the light in vacuum, and θ is the scattering angle. For room temperature scattering measurements for which data are taken over a range of wavevectors, D_m is obtained through a linear fit of $\bar{\Gamma}$ vs q^2, with imposed zero intercept.

In the dilute limit, D_m can be approximated by the tracer diffusion coefficient, D_t, and it then possible to use the Stokes−Einstein equation to determine the apparent hydrodynamic radius

$$R_h = \frac{k_B T}{6\pi\eta D_t} \tag{2}$$

where k_B is the Boltzmann constant, T is the absolute temperature, and $\eta(T)$ is the viscosity of the solvent. The temperature dependence of the viscosity has been reported to be well-described by the Vogel−Fulcher−Tamman equation for both ionic liquids.[44,45]

The distribution of aggregate sizes was also evaluated by applying a regularized inverse Laplace transformation to the dynamic light scattering data using the REPES algorithm.[46] The decay rate distribution obtained, $G(\Gamma)$, can then be transformed to a hydrodynamic radius distribution using eq 2. When the size distribution obtained through the REPES routine displayed a bimodal distribution, consistent with a high $\mu_2/\bar{\Gamma}^2$ value from the cumulant method, the experimental squared electric field correlation function was fit to a double-exponential function to extract the average decay rates from the two distinct particle distributions.

$$g_1(t) = A_1\exp(-\bar{\Gamma}_1 t) + A_2\exp(-\bar{\Gamma}_2 t) \tag{3}$$

Small-Angle Neutron Scattering (SANS). SANS experiments were performed on the NG-7 30 m instrument of the Cold Neutron Research Facility at the National Institute of Standards and Technology (NIST). The block copolymer solutions described previously were placed in quartz banjo cells with a path length of ~1.1 mm and were heated to the desired temperature by placing the cells in a heating block. A sample-to-detector distance of 13 m with a monochromated neutron wavelength $\lambda = 6$ Å, and a wavelength spread of $\Delta\lambda/\lambda = 0.11$, were used to cover a scattering wave vector range $q = 0.0036-0.049$ Å^{-1}. Here, the scattering vector is defined as $q = (4\pi/\lambda)\sin(\theta/2)$. The two-dimensional scattering spectra obtained were reduced by azimuthal integration to yield intensity vs q data. The raw data were corrected for background detector efficiency, empty cell scattering, and sample transmission and then converted to absolute intensity with direct beam flux measurements. Finally, incoherent scattering from the solvent was subtracted.

Results and Discussion

Path Dependence of Micellar Morphology. *BO(8−7)/[EMI][TFSI]*. It has been established that PB−PEO block copolymers can self-assemble into micelles when dissolved in [EMI][TFSI], forming aggregates with a PB core and a well-solvated PEO corona.[31,36,42] In a recent communication,[31] we probed the path dependence of the aggregate morphologies assumed by the BO(8−7) block copolymer in [EMI][TFSI]. We demonstrated that for this system DD preparation methods typically produce large and polydisperse micellar structures. The values of the average hydrodynamic radius and polydispersity of an “as-prepared” micellar solution, $\langle R_h\rangle_0$ and $\langle\mu_2/\bar{\Gamma}^2\rangle_0$, obtained from DLS measurements are reproduced in Table 2.

The formation of aggregates that lie far from equilibrium is not uncommon for DD preparation protocols, particularly for a polymer in which the insoluble block represents a large fraction of the total size of the block copolymer. The limited solubility of the polymer chain is expected to lead to a micellization scenario in which the nucleation of micelles is overcome by the speed of micellar growth, resulting in large and polydisperse aggregates. It has also been suggested that the morphology of micelles prepared through DD might depend not only on the properties of the selective solvent but also on the morphology of the bulk polymer as well. That is, the solid copolymer should swell when placed in contact with the selective solvent and might then break into pieces forming micelles with sizes that should be commensurate with the original domain size.[6,47] In this case, BO(8−7) presents a lamellar morphology in the bulk with a domain spacing of 27 nm (see Supporting Information), i.e., about half of the size of the DD-prepared micelles.

Upon thermal treatment at 170 °C, however, these metastable aggregates evolved into a steady-state morphology of monodisperse micelles (Table 2). Cryo-TEM images of the DD micelles after thermal treatment confirmed the spherical morphology of these aggregates (see Supporting Information). The evolution of $\langle R_h\rangle(t)$ could be followed using DLS, where the micelle size was seen to decay with time until a steady-state value of $\langle R_h\rangle_f \approx 29$ nm was attained.[31] Figure 1a shows the normalized relaxation functions, namely, $R(t) = [\langle R_h\rangle(t) - \langle R_h\rangle_f]/[\langle R_h\rangle_0 - \langle R_h\rangle_f]$ versus t, in a semilog

Table 2. Apparent Hydrodynamic Radii and Size Distribution of the Block Copolymer Micelles in Ionic Liquids at a Concentration of 0.5 wt %[a]

		as-prepared		steady-state[b]	
solution	preparation procedure	$\langle R_h \rangle_0$ (nm)[c]	$\langle \mu_2/\bar{\Gamma}^2 \rangle_0$	$\langle R_h \rangle_f$ (nm)[c]	$\langle \mu_2/\bar{\Gamma}^2 \rangle_f$
BO(8−7)/[EMI][TFSI]	DD	54	0.27	29	0.08
	CS	16	0.10	15	0.07
BO(8−15)/[EMI][TFSI]	DD	34	0.06	29	0.06
	CS	16	0.07	17	0.07
BO(8−7)/[BMI][TFSI]	DD	108	0.54	31	0.01
	CS	18	0.02	17	0.05
SO(11−10)/[EMI][TFSI]	DD	480/60[d]	0.9	33	0.17
	CS	15	0.07	15	0.08

[a] All DLS measurements were taken at 25 °C. [b] Solutions labeled "steady-state" were obtained after thermal annealing at 170 °C. [c] Hydrodynamic radii calculated from linear fits of Γ vs q^2 plots, where Γ is obtained by fitting correlation functions with the cumulant expansion (eq 1). [d] $\langle R_h \rangle$ obtained by fitting the correlation function with the double exponential function (eq 3).

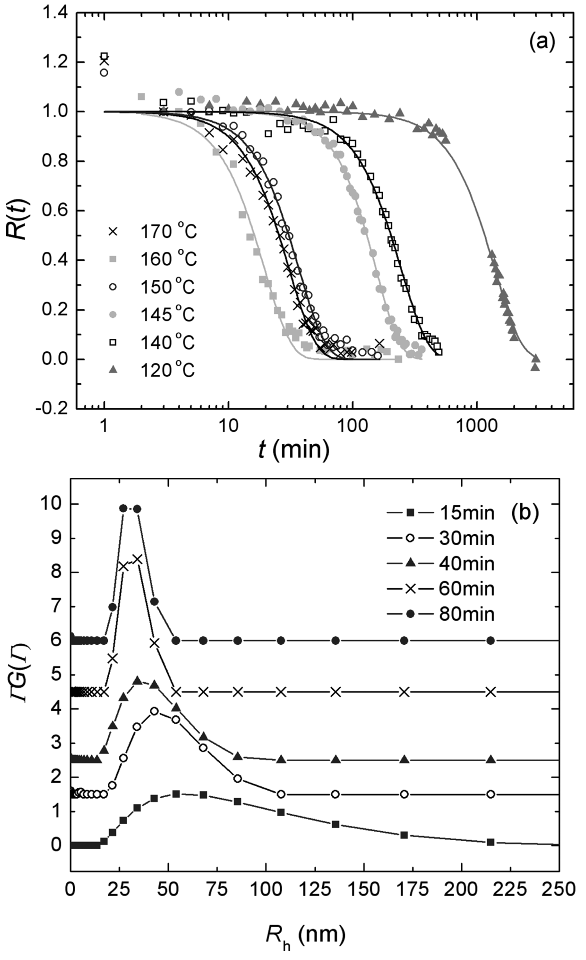

Figure 1. (a) Time dependence of the normalized hydrodynamic radius for 0.5 wt % DD solutions of BO(8−7) in [EMI][TFSI] at different relaxation temperatures and a 90° scattering angle. The lines show compressed exponential fits of the dynamic traces with a fixed exponent, $n = 2$. (b) Evolution of the hydrodynamic radius distribution as a function of annealing time ($T = 170$ °C, $\theta = 90°$).

scale for various annealing temperatures. Concomitant to the clear decrease in micelle size, there is a gradual decrease in the polydispersity of the micelle size. This is illustrated in Figure 1b, where the time-dependent size distributions obtained from the REPES routine are shown for relaxation at 170 °C. The extremely broad distributions obtained at earlier times are seen to shift gradually to smaller R_h values with annealing time, becoming more narrow and symmetric in the process.

The dynamics of the structural relaxation will be examined in further detail in the next section. However, it is important to mention that the steady-state size of the micelles was shown to be insensitive to the annealing temperature in the thermal relaxation experiment, wherein a constant $\langle R_h \rangle_f$ was obtained after annealing over a wide temperature range (from 120 to 180 °C).[44] Also, while the value of $\langle R_h \rangle_0$ varied significantly when repeating the preparation of the DD solution, as one might expect for a nonequilibrium system, the same final micelle size was always recovered upon thermal treatment of any DD solution. This suggests (but does not prove) that the micelles may be close to their equilibrium size.

In contrast, the CS method, in which the solvent quality is gradually varied to allow aggregation of the core-forming block, was shown to yield consistently smaller spherical micelles (see Supporting Information) with a narrow distribution of aggregate sizes that remained unchanged upon extended thermal treatment (Table 2). These micelles were about half the size of the annealed DD micelles, $\langle R_h \rangle_f = 15$ nm. Thus, control of the block copolymer assembly and relaxation pathways can lead to two distinct yet narrow distributions of steady-state aggregates with significantly different average sizes, but the same morphology, i.e., spherical micelles. This is better captured in a comparison of the steady-state micellar size distributions for both preparation procedures, displayed in Figure 2a.

It is interesting to point out that micelles prepared with the CS methodology using tetrahydrofuran as the cosolvent yielded very similar size distributions as those obtained with dichloromethane (results not shown). This demonstrates that preferential solvation of the PEO block by the chlorinated solvent[48] is not a major factor in determining the morphology of the CS micelles.

The results obtained highlight the difficulty of distinguishing an equilibrium morphology from a metastable one in highly amphiphilic diblock copolymer dispersions. On the basis of the evidence indicating that DD-prepared micelles might be relaxing to sizes close to the equilibrium micelle size, we previously concluded that CS-prepared micelles must be a long-lived metastable morphology.[31] This is in agreement with reports from Zhang and Eisenberg,[49] who studied how the morphological transitions of crew-cut aggregates from polystyrene-*b*-poly(acrylic acid) diblock copolymers in DMF/water mixtures depend on the method of aggregate formation. Specifically, they demonstrated that under certain water concentrations and using a direct dissolution method they are able to observe reversible morphological transitions that are unachievable when the aggregates are prepared through a water addition method (analogous to the CS method), due to kinetic entrapment.

BO(8−15)/[EMI][TFSI]. We tested whether thermodynamic equilibrium can be more readily achieved in DD micelles if the overall solubility of PB−PEO copolymer

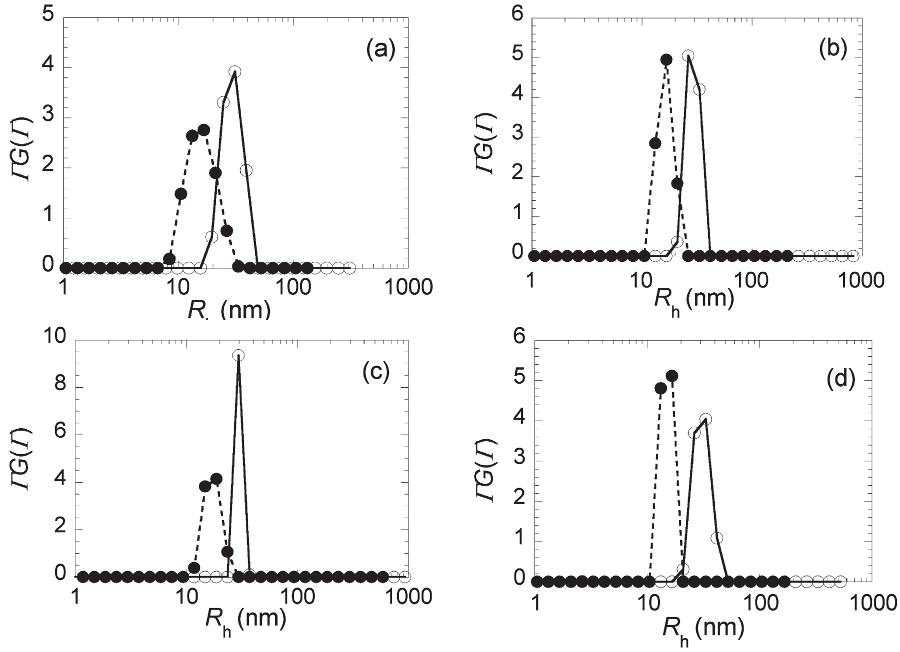

Figure 2. Hydrodynamic radius distributions obtained by applying the Laplace inversion routine REPES to correlation data obtained from DLS measurements at a fixed scattering angle. Two distinct yet narrow distributions are obtained in a variety of block copolymer systems in ionic liquids using DD (open symbols) and CS preparation protocols (filled symbols) after annealing at 170 °C. (a) BO(8−7) in [EMI][TFSI], (b) BO(8−15) in [EMI][TFSI], (c) BO(8−7) in [BMI][TFSI], and (d) SO(11−10) in [EMI][TFSI].

chains in the ionic liquid is increased. The enhanced solubility should allow a more controlled growth of micelles and lessen any influence of the bulk polymer morphology on the structure of the "as-prepared" micelles. Thus, we increased the degree of polymerization of the PEO block while maintaining a constant PB chain length, such that the block copolymer was more easily dissolved in [EMI][TFSI]. Indeed, micelles that were prepared with a BO(8−15) copolymer via the DD method were on average smaller and more narrowly distributed than their BO(8−7) counterparts (Table 2). Moreover, upon thermal relaxation at 170 °C the average aggregate size changed by only a few nanometers, while maintaining a similar degree of polydispersity. The small variations in size encountered upon annealing are another indication that thermodynamics of aggregation control the formation of DD-micelles in this system. That is, micelles with aggregation numbers close to the equilibrium value are obtained after preparation, without the need of extended thermal annealing. This result is not unexpected for starlike micelles, where the core chain is small with respect to the size of the corona chain.[6] In comparison, the micelles prepared with the BO(8−15) copolymer using the CS methodology were again approximately half the size of the corresponding DD-prepared aggregates (Table 2). As with the BO(8−7) polymer, the thermal relaxation experiments performed with the BO(8−15) CS solution at 170 °C revealed that $\langle R_h\rangle$ and $\langle \mu_2/\overline{\Gamma}^2\rangle$ remained approximately constant over a period of 43 h. Consequently, the narrow, steady-state size distributions obtained via the CS and DD preparation procedures demonstrate once again a striking difference in the size of the aggregates (Figure 2b), where the CS-prepared micelles are suspected to represent a metastable morphology.

We propose the following qualitative explanation for kinetic entrapment of these micelles. In the CS preparation protocol, block copolymer chains are initially molecularly dissolved in a good solvent mixture. The evaporation of the cosolvent will gradually make the solvent mixture more selective toward the PEO block, prompting the PB blocks to aggregate into micelles. For the BO(8−15) copolymer, the cmc is reached at a dichloromethane concentration of roughly 32 wt %, as measured using DLS (see Supporting Information). Chain exchange should be rapid at these high cosolvent concentrations, when the cores are swollen with dichloromethane and the core/solvent incompatibility is weak.[6] At this stage, thermodynamics will dictate the evolution of the system. As cosolvent evaporation proceeds, the micelles are expected to grow since the aggregation number should increase with increasing core−solvent interfacial tension. However, as the quality of the solvent becomes progressively poorer for the core block and the concentration of unimers in solution decreases, chain exchange will slow down and the morphology will eventually be locked in. The polydispersity of the resulting micellar size distribution should be fairly narrow, reflecting thermodynamic equilibration at the onset of micelle formation, but the average micelle size will be less than the equilibrium value in pure ionic liquid.

BO(8−7)/[BMI][TFSI]. In an alternate strategy to increase the copolymer solubility, we replaced [EMI][TFSI] with another imidazolium-based ionic liquid, [BMI][TFSI]. The two ionic liquids differ only in the size of the pendant alkyl chain from the imidazolium cation. The increase in alkyl chain length should enhance dispersive interactions with the PB chains and consequently decrease the selectivity of the solvent. This hypothesis is supported by the smaller difference between the solubility parameters of [BMI][TFSI] and PB ($\delta_{[BMI][TFSI]} = 26.7$ MPa$^{1/2}$, $\delta_{PB} = 17.1$ MPa$^{1/2}$) than that between [EMI][TFSI] and PB ($\delta_{[EMI][TFSI]} = 27.6$ MPa$^{1/2}$).[50,51] The change of solvent should then lead to a lower interfacial tension between the nonpolar core and the solvent, presumably resulting in more rapid equilibration kinetics. The results obtained from the BO(8−7)/[BMI][TFSI] system are qualitatively similar to BO(8−7)/[EMI][TFSI] (Figure 2c). Namely, the DD preparation protocol led to extremely large and polydisperse structures ($\langle R_h\rangle_0 \approx$ 100 nm) that relaxed onto smaller, monodisperse micelles

($\langle R_h \rangle_f$ = 31 nm) upon thermal treatment (Table 2). On the other hand, the smaller micelles obtained via CS-aided aggregation remained unaltered by prolonged thermal annealing ($\langle R_h \rangle_0$ = 16 nm, $\langle R_h \rangle_f$ = 17 nm). It is interesting to note that neither the kinetic pathways of micelle formation nor the final average size of the micelles seemed to vary significantly when switching to a less selective solvent, presumably because the difference in selectivity of the two solvents toward PB is not large. The difference in relaxation kinetics for the two solvents will be discussed in a subsequent section.

SO(11−10)/[EMI][TFSI]. We modified the nature of the core-forming block in a further effort to probe the development of the two path-dependent micellar distributions. The polymer chosen, SO(11−10), was a PS−PEO diblock copolymer with a weight fraction of PEO and total degree of polymerization comparable to BO(8−7). On one hand, the compatibility between the insoluble PS block and the ionic liquid is expected to be greater than that of PB and [EMI][TFSI], judging from the slightly more polar nature of PS. Once again this conjecture is supported by comparing the solubility parameters of both core blocks with that of the ionic liquid (δ_{PS} = 18.6 MPa$^{1/2}$ and δ_{PB} = 17.1 MPa$^{1/2}$).[51] On the other hand, the high glass transition temperature, T_g, of PS will undoubtedly restrict the mobility of the core chains, possibly leading to frozen micellar structures during aggregate formation. Indeed, DLS measurements of the as-prepared DD solution revealed the presence of very large aggregates with polydispersities nearing 0.9. In fact, the R_h distribution obtained from the REPES routine clearly showed the existence of two distinct peaks (see Supporting Information). By refitting the data with a double-exponential function (eq 3), we were able to obtain the $\langle R_h \rangle_0$ of each peak, as shown in Table 2. The formation of frozen PS−PEO aggregates in aqueous solutions displaying multimodal micellar distributions has been extensively reported in the literature.[52,53] The peaks corresponding to larger R_h values have often been attributed to secondary association of aggregates or loose micellar clusters.

Upon annealing the DD solutions at 170 °C, the size of the aggregates decreased almost instantaneously to $\langle R_h \rangle_f \approx$ 33 nm. In fact, the time scales associated with the relaxation process were too short to follow the change in micelle size with DLS over the temperature range studied. When the micellar solution is annealed at temperatures above the T_g of PS, the rapid evolution is consistent with a significantly diminished incompatibility between the core-forming block and the solvent, as compared to the BO(8−7)/[EMI][TFSI] system. During this evolution, the aggregate size distribution becomes monomodal and the width of the distribution is greatly reduced (Figure 2d).

Again, the CS-prepared micelles for SO(11−10) were appreciably smaller than their DD counterparts and preserved their original size and width of distribution throughout the long annealing process at high temperatures (Table 2). The consistent formation of two path-dependent, steady-state, micellar size distributions obtained in copolymers with varying soluble block weight fractions, chemistries of the ionic liquid cation, and even chemistry of the core block (Figure 2) suggests a fundamental difference in the active mechanisms of micelle formation and relaxation that presumably allows the morphology of DD-prepared micelles to be dictated by thermodynamics but prevents CS-micelles from equilibrating even upon extended thermal annealing.

Relaxation Kinetics of DD-Prepared Micelles in Ionic Liquids. We now focus on the time dependence of the scattered intensity by DD micelles prepared with the BO(8−7) copolymer in [EMI][TFSI], after temperature jumps from 25 °C to final temperatures between 120 and 170 °C. As mentioned earlier, Figure 1a shows the normalized relaxation functions at various temperatures. It is clear that the overall shape of the decay curves is similar throughout the temperature range studied. Specifically, at short times there is a plateau region where $R(t) \approx R(t=0)$, followed by a sharp decrease in micelle size until the steady-state size is attained at long times. The characteristic relaxation time, τ, and the extent of the plateau region increase with decreasing temperature. However, it is important to re-emphasize that all experiments lead to approximately the same final micelle size, $\langle R_h \rangle_f \approx$ 30 nm.

Table 3. Characteristic Times for Equilibration of DD-Prepared Micelles as a Function of Temperature

	BO(8−7)/[EMI][TFSI]			BO(8−7)/[BMI][TFSI]		
T (°C)	η (kPa·s)[a]	τ (s)[b] × 10^{-3}	R^2	η (kPa·s)[a]	τ (s)[b] × 10^{-3}	R^2
120	4.2	83	0.996			
140	3.3	15	0.985	3.7	30	0.954
145	3.1	9.3	0.994	3.5	18	0.965
150	2.9	2.2	0.989	3.3	11	0.973
155				3.1	15	0.991
160	2.6	1.2	0.982	3.0	13	0.992
170	2.4	1.8	0.982	2.7	5.2	0.988

[a] Estimated using the VFT equation with the parameters reported in refs 44 and 45. [b] Obtained by fitting dynamic traces to a compressed exponential function (eq 4) with n = 2.

We attempted to fit $R(t)$ to single-exponential as well as double-exponential decay functions. The latter typically led to characteristic relaxation times with large standard errors and amplitudes for the two processes that had opposite signs, which is physically unreasonable (see Supporting Information for an example). On the other hand, the quality of the fits with the single-exponential decay function was consistently poor, as exemplified in the last figure of the Supporting Information, where the fit to the experimental data at 140 °C, along with a plot of the residuals vs time, is shown. In fact, examination of this plot shows that $R(t)$ decays significantly more rapidly than a single-exponential function. Similar results were obtained for all temperatures studied. This prompted us to try to fit the dynamic traces to an Avrami-type equation of the form

$$R(t) = \exp[-(t/\tau)^n] \tag{4}$$

where τ is the characteristic relaxation time and the exponent $n > 1$. The data are shown to fit nicely to this "compressed exponential" function[54] over the temperature range studied, as represented in Figure 1a. This is also observed from the R^2 values of the fitting results, which are all greater than 0.98 (Table 3).

The fits with eq 4 were initially performed allowing two adjustable parameters, τ and n, where the average value of the exponent was found to be equal to 2.03 ± 0.18. Refitting all the data with a fixed exponent value n = 2 (Figure 1a) yielded similar quality fits with little change in the τ values extracted. The relaxation times thus obtained were strongly dependent on temperature, with characteristic time scales spanning an order of magnitude ($\tau(T) = (1-83) \times 10^3$ s, see Table 3). It is important to note that these relaxation times are several orders of magnitude larger than the time required for thermal equilibration of the sample, which we estimate to be on the order of a minute at the lowest temperature probed.

Dynamic traces for DD-prepared micelles from the BO(8−7)/[BMI][TFSI] system as a function of temperature were

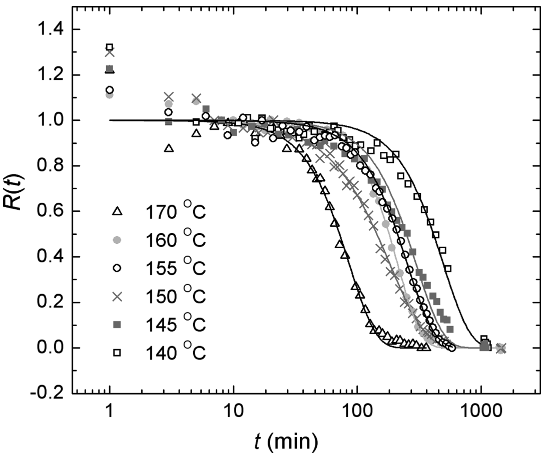

Figure 3. Time dependence of the normalized hydrodynamic radius for 0.5 wt % solutions of BO(8−7) in [BMI][TFSI] at different relaxation temperatures and a 90° scattering angle. The lines represent compressed exponential fits of the dynamic traces with $n = 2$.

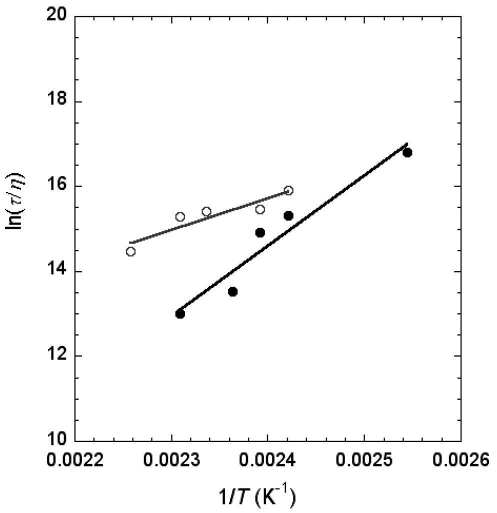

Figure 4. Arrhenius plot of τ obtained for the equilibration of micelles prepared with the BO(8−7) copolymer using the DD procedure in [EMI][TFSI] (filled) and in [BMI][TFSI] (open).

also obtained. The traces were also well fitted with eq 4 with an exponent $n = 2$ (Figure 3). However, in this system the calculated decays showed comparatively larger deviations from the data at short annealing times ($t < 10$ min) than observed for the same copolymer in [EMI][TFSI]. This is possibly indicative of an additional, faster relaxation process not resolved in the BO(8−7)/[EMI][TFSI] system. The relaxation times obtained are roughly comparable to those obtained in [EMI][TFSI] (($\tau(T) = (5-30) \times 10^3$ s, see Table 3), yet it is important to remember that the initial size of the as-prepared micelles was much larger in [BMI][TFSI] (Table 2).

The activation energy of the relaxation process can be estimated from the temperature dependence of the relaxation times. In the Arrhenius plot presented in Figure 4 the significant temperature dependence of the viscosity of the ionic liquids is accounted for by taking the ratio $\tau(T)/\eta(T)$. Activation energies of approximately 140 and 60 kJ/mol were calculated for the relaxation of the DD micelles in [EMI][TFSI] and [BMI][TFSI], respectively. While the approach to calculating the activation energies is empirical in nature, the results obtained are in accordance with the expectation that the ionic liquid with the longer alkyl chain should be more compatible with the core block and therefore lead to a lower energy barrier to equilibration.

Table 4. Characteristic Times for Equilibration of DD-Prepared Micelles at 170 °C as a Function of Concentration for BO(8−7)/[EMI][TFSI]

concentration (wt %)	$\langle R_h \rangle_0$ (nm)	$\langle \mu_2/\overline{\Gamma}^2 \rangle$	τ (s)[a] × 10^{-3}	R^2
1.0	91	0.45	1.6	0.987
0.50	76	0.45	11	0.994
0.25	75	0.38	15	0.994
0.10	72	0.36	17	0.989
0.05	64	0.37	15	0.972

[a] Obtained by fitting dynamic traces to a compressed exponential function (eq 4) with $n = 2$.

As a reference, if we assume that the micelles relax via single insertion/expulsion mechanism in which the exchange is controlled through diffusion of a chain through the core with an enthalpic penalty for crossing the interface, i.e., a hindered diffusion mechanism,[55−58,27] then the diffusion coefficient will be given by

$$D D_0 \exp[-\alpha\chi N_{\mathrm{core}}] \tag{5}$$

where χ is the interaction parameter between the solvent and the core, D_0 is the diffusion coefficient in the absence of any interactions, and α is a prefactor of order unity. The activation barrier should then scale as $E_a/RT \sim \alpha\chi N_{\mathrm{core}}$, yielding values of $\chi_{\mathrm{EMITFSI\text{-}PB}} = 0.22$ and $\chi_{\mathrm{BMITFSI\text{-}PB}} = 0.10$ at 170 °C. These χ values are somewhat smaller than expected if, for example, we compare them to reported χ values of the same polymer in water ($\chi_{\mathrm{PB\text{-}H_2O}} = 3.5$ at 25 °C)[59] and shed some doubt to the idea that the mechanism of relaxation is single insertion/expulsion.

To gain further insight into the mechanism of micelle equilibration, the concentration of the BO(8−7) copolymer in [EMI][TFSI] was varied from 0.05 to 1.0 wt %. The concentration series was made by dilution of a 1 wt % solution prepared through the DD procedure as described in the Experimental Section. The dilution process led to a significant decrease in $\langle R_h \rangle_0$, as shown in Table 4. Nevertheless, thermal relaxation of the micellar solutions at 170 °C resulted in a constant $\langle R_h \rangle_f \cong 30$ nm for all concentrations.

As before, the dynamic traces were well-fit with the Avrami equation (Figure 5a) with a fixed exponent, $n = 2$ ($\langle n \rangle = 2.25 \pm 0.16$ when free-fitting τ and n), leading to τ values in the range of $(1-15) \times 10^3$ s (Table 4). Figure 5b demonstrates that there is a clear decrease in the relaxation time with increasing concentration, despite the fact that τ might be expected to increase with increasing $\langle R_h \rangle_0$. The concentration dependence of τ is particularly strong for concentrations greater than 0.25 wt %. Such a concentration dependence has been typically attributed to a fusion/fission mechanism,[18,19,60] since the collision between aggregates is expected to yield second-order kinetics.[10] These results prompted us to measure the rates of single chain exchange directly to further confirm the mechanism by which DD-prepared micelles equilibrate.

SANS Measurements of Single Chain Exchange Kinetics. SANS experiments were performed to explore the steady-state chain exchange kinetics between PB−PEO diblock copolymer micelles dispersed in [EMI][TFSI]. The underlying concept is to mix two (nearly) identical populations of micelles that differ only in the isotopic labeling of the core chains and determine the rate of chain exchange as the micelles hybridize at equilibrium. Hybridization is followed by measuring the change in scattering intensity with time,[20,24−27,61] which is related to the difference in scattering length density (SLD) between the core and the solvent, $I(q)^{1/2} \sim \mathrm{SLD_{core}}(t) - \mathrm{SLD_{solv}}$. The scattering

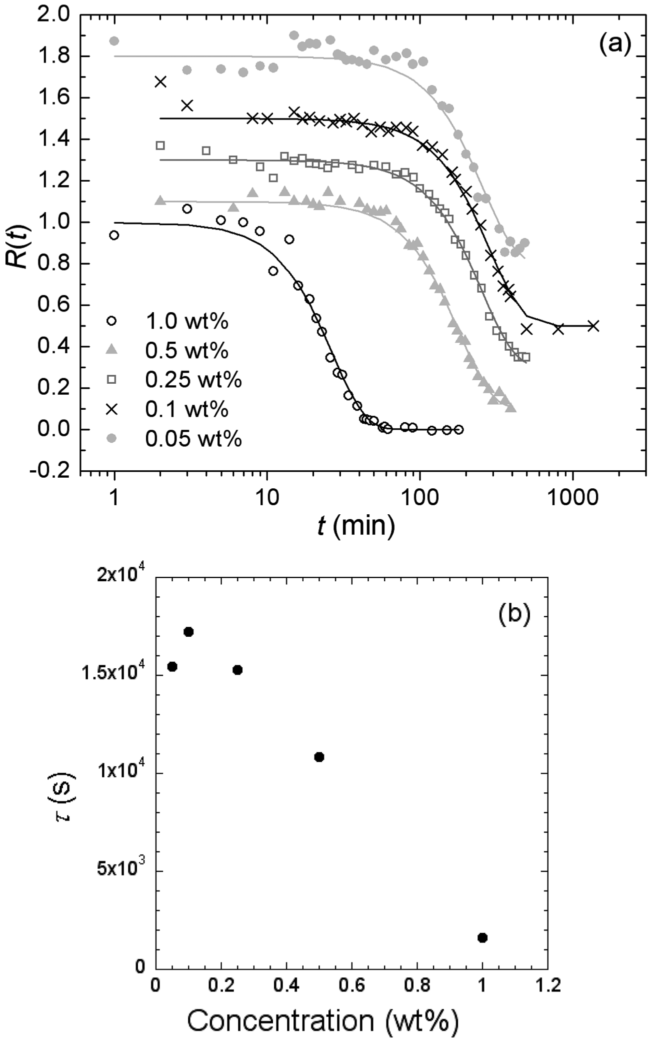

Figure 5. (a) Time dependence of the normalized hydrodynamic radius of BO(8−7) micelles in [EMI][TFSI] at different concentrations and a 90° scattering angle. The lines show the fitting of the relaxation data with compressed exponential functions (n = 2). The data have been shifted in the y-axis for clarity. (b) Concentration dependence of the relaxation time for solutions of BO(8−7) in [EMI][TFSI].

from the corona chains is expected to remain constant throughout the experiment. The scattered intensity of a postmixed solution should be maximal at $t = 0$, when the micelles with protonated (hPB) and deuterated (dPB) cores are segregated, and should decrease as chains are exchanged between the micelles until complete hybridization is attained. This becomes clear when comparing the core contrast from background of the two types of micelles ($\mathrm{SLD_{hPB}} = 4.03 \times 10^9$ cm^{-2}, $\mathrm{SLD_{dPB}} = 64.6 \times 10^9$ cm^{-2}, and $\mathrm{SLD_{[EMI][TFSI]}} = 24.2 \times 10^9$ cm^{-2}) with that of a hybridized micelle, for which $\mathrm{SLD_{hPB+dPB}} = (\mathrm{SLD_{hPB}} + \mathrm{SLD_{dPB}})/2 = 34.3 \times 10^9$ cm^{-2}. It is important to note that the scattering profile of a completely randomized postmixed sample should be identical to that of the premixed sample, where the two polymers are blended prior to making the micellar solution, providing a benchmark to determine whether hybridization of the micelles occurs.

Before performing the SANS experiments, we measured the size of the micelles using DLS to corroborate that deuterated and protonated aggregates prepared with the same methodology had a similar micelle size. Table 5 shows a good agreement between the sizes of hPB−PEO and dPB−PEO micelles in each preparation protocol. The DD-prepared micelles were then annealed at 145 °C for 30 h to ensure that the steady-state morphology was attained.

Table 5. Size and Polydispersity of Block Copolymer Micelles Formed at a Concentration of 1 wt % in [EMI][TFSI] for SANS Measurements

polymer	preparation procedure	$\langle R_h \rangle$ (nm)	$\langle \mu_2/\Gamma^2 \rangle$
BO(8−20)	DD[a]	37	0.20
dBO(7−28)	DD[a]	35	0.27
BO(8−20)	CS	20	0.16
dBO(7−28)	CS	20	0.18

[a] DD solutions were annealed at 145 °C for 30 h.

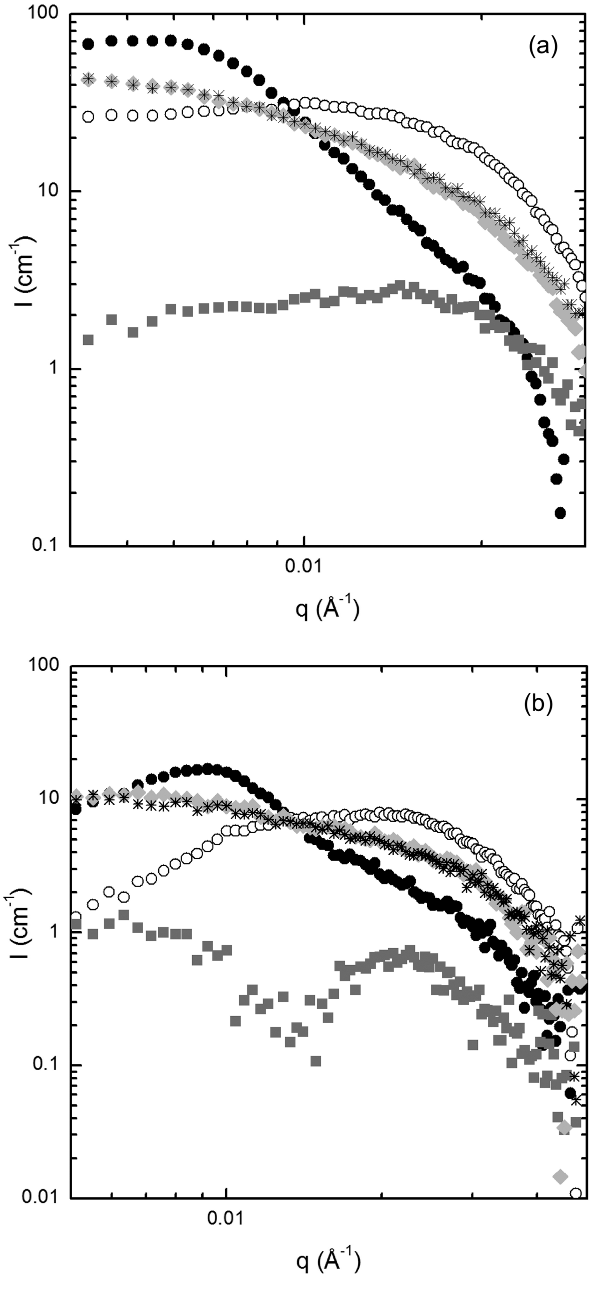

Figure 6. SANS patterns of 1 wt % solutions of dBO(7−28) (open circles) and BO(8−20) (filled circles) micelles in [EMI][TFSI] at 20 °C as well as premixed (gray squares) and postmixed solutions (t = 0, gray diamonds) of the two copolymers prepared through (a) direct dissolution and (b) cosolvent dissolution. The scattering data of the postmixed solutions after 2 h of annealing at 200 °C are also shown (black crosses).

Figure 6a displays the individual SANS profiles for micelles of dBO(7−28) and BO(8−20) prepared through DD as well as that of a postmixed sample of the two, immediately after mixing (t = 0). As expected, the intensity profile of the latter is well-represented by the arithmetic mean of the individual profiles of dBO(7−28) and BO(8−20).[61] Moreover, the figure demonstrates that the scattering intensity from the DD-premixed sample is substantially diminished as compared to that of the postmixed sample at t = 0, as anticipated from the scattering length densities of the polymers.

After preparation, the DD-postmixed sample was subjected to a temperature ramp from 20 to 200 °C, taking measurements at 15 min intervals, after which the sample was held at 200 °C for 1 day. Figure 6a shows that the scattering intensity of the postmixed sample did not decrease measurably after 2 h of annealing at 200 °C, retaining its shape with the extended thermal treatment. In fact, the scattering curve remained identical even after 24 h of annealing at this temperature (not shown). These results indicate that no chain exchange occurs between the micelles and, consequently, that the steady-state, DD-prepared aggregates can be regarded as kinetically frozen. Qualitatively similar results are obtained for the CS-prepared micelles, as observed in Figure 6b, revealing that these aggregates are also kinetically trapped.

It is necessary to mention that some degradation of the copolymer does occur after prolonged annealing at 200 °C, as observed from the formation of a gel-like material at very long times. However, the scattering intensity profiles of Figure 6 were taken well before the sample showed visible signs of degradation. Moreover, our results are in accordance with similar SANS experiments reported by Won et al.,[61] who demonstrated that aqueous solutions of sphere-forming PB−PEO diblock copolymers with a PB chain length ($N_{\mathrm{core}} \sim 70$) were kinetically frozen on time scales of days at room temperature. The unfavorable thermodynamic interactions between core and solvent are assumed to be somewhat stronger in aqueous based mixtures than in the ionic liquid mixture, as predicted by their solubility parameters ($\delta_{[\mathrm{EMI}][\mathrm{TFSI}]} = 27.6\ \mathrm{MPa}^{1/2}$, $\delta_{\mathrm{H_2O}} = 47.9\ \mathrm{MPa}^{1/2}$). Thus, a stronger segregation and slower dynamics are expected in the former system for the same PB−PEO block copolymer. However, the rate of chain exchange has been shown to be extremely sensitive to size of the insoluble block,[27] where a moderate increase in N_{core} (∼60% increase) can lead to relaxation times that are several orders of magnitude longer than those observed in the copolymer with a shorter core block. The steep dependence of the exchange dynamics on N_{core} is a consequence of the barrier to escape of core blocks (eq 5). In our SANS experiments the length of the PB block is about twice the size ($N_{\mathrm{d\text{-}core}} \sim 122$, $N_{\mathrm{h\text{-}core}} \sim 146$) of the PB−PEO diblock copolymer studied in ref 61, which explains the lack of exchange observed in our experiments.

On the basis of these SANS results, it is reasonable to assume that single chain exchange between micelles prepared with the BO(8−7) copolymer should also be highly restricted, and therefore, the relaxation observed for DD micelles must be attained through some form of fusion/fission mechanism. However, the question of why this equilibration (or partial equilibration) can be accomplished by annealing the DD-prepared micelles, but not the CS-prepared ones, still remains. We propose that equilibration (or partial equilibration) is achievable in the former because fusion and fission are more likely to occur when the aggregation number of a micelle (Q) is far from the equilibrium aggregation number (Q_{eq}), as suggested by Dormidontova.[13] The free energy analysis she presents demonstrates that fission into equally sized micelles is the most efficient way of lowering the free energy of a micellar solution when $Q > 1.5Q_{\mathrm{eq}}$. However, the long time scales associated with the fission of large micelles suggest that emission of small micelles, followed by the coupling of these small aggregates, is a more likely route. The BO(8−7) and SO(11−10) block copolymers studied in this work form extremely large and polydisperse micelles after preparation through the DD protocol and may thus be prone to equilibration by such a mechanism. On the other hand, according to Dormidontova, there is a logarithmic time dependence for the growth of Q through aggregate fusion due to an increase in the activation energy for fusion of larger micelles. Thus, the process of fusion of two averaged-sized micelles resulting in the doubling of Q is highly favored when these micelles are relatively small but becomes inactive when $Q > Q_{\mathrm{eq}}^{5/9}$, whereas the fusion of unequally sized micelles is expected to contribute even in later stages of micellar growth. Cryo-TEM measurements[31] showed that the aggregation number of the CS micelles is narrowly distributed around an average value of $Q_{\mathrm{CS}} \approx 130$, while the steady-state DD micelles, which we assume have achieved an aggregation number close to equilibrium, have $Q_{\mathrm{DD}} \approx Q_{\mathrm{eq}} \approx 950$. Accordingly, CS-prepared micelles may not be sufficiently far from equilibrium to allow fusion of average-sized micelles ($Q_{\mathrm{eq}}^{5/9} \approx 45$) and too narrowly distributed to allow any fusion event at all.

Conclusions

We have investigated the path dependence of the morphology of highly amphiphilic diblock copolymer micelles in imidazolium-based ionic liquids. Specifically, we have confirmed that CS and DD preparation protocols can lead to two narrow, but substantially different, steady-state distributions of PB−PEO micellar sizes, as was indicated in a previous report. The two distributions were consistently observed upon high-temperature annealing after modifying the length of the corona chain and the length of the pendant alkyl chain in the imidazolium cation and even upon changing the chemistry of the core block to PS. This clearly demonstrates that the active mechanisms of micelle formation and relaxation in DD-prepared micelles are fundamentally different from those in CS micelles. Remarkably, measurements of the kinetics of micelle relaxation reveal that DD micelles relax faster than exponentially, having dynamic traces that are well-fit by an Avrami-type equation. To our knowledge, there is no theoretical framework that would explain such a fast decay in the evolution of micelles size. In addition, it is shown that the relaxation times obtained decrease with increasing concentration. This result, along with ancillary SANS measurements that establish that single chain exchange between micelles is severely restricted in PB−PEO micelles, led us to believe that relaxation of DD micelles toward the equilibrium aggregation number is accomplished through fusion/fission. We propose that relaxation of micelles through a fusion/fission mechanism is only possible for as-prepared DD micelles, and not for CS micelles, because the initial size distribution of the former is polydisperse and lies far from equilibrium.

Acknowledgment. This work was supported primarily by the MRSEC program of the National Science Foundation under Awards DMR-0212302 and DMR-0819885 and by the University of Minnesota through an MSROP fellowship (J.M.S.). Sangwoo Lee and Dr. Huiming Mao kindly provided the block copolymers used in this study, and Lizbeth Esquivel and Dr. Lei Zhang assisted with the measurements of micellization in mixed solvents.

Supporting Information Available: Additional SAXS, cryo-TEM, and DLS characterization of block copolymers and their micelles in ionic liquids. This material is available free of charge via the Internet at http://pubs.acs.org.

References and Notes

(1) Hubbell, J. A. *Science* **2003**, *300*, 595.
(2) Meier, W. *Chem. Soc. Rev.* **2000**, *29*, 295.
(3) Jung, H. M.; Price, K. E.; McQuade, D. T. *J. Am. Chem. Soc.* **2003**, *125*, 5351.
(4) Vriezema, D. M.; Aragones, M. C.; Elemans, J. A. A. W.; Cornelissen, J. J. L. M.; Rowan, A. E.; Nolte, R. J. M. *Chem. Rev.* **2005**, *105*, 1445.
(5) Jain, S.; Bates, F. S. *Macromolecules* **2004**, *37*, 1511.
(6) Cameron, N. S.; Corbierre, M. K.; Eisenberg, A. *Can. J. Chem.* **1999**, *77*, 1311.
(7) Jain, S.; Bates, F. S. *Science* **2003**, *300*, 460.
(8) Cui, H.; Chen, Z.; Zhong, S.; Wooley, K. L.; Pochan, D. J. *Science* **2007**, *317*, 647.
(9) Smith, C. K.; Liu, G. *Macromolecules* **1996**, *29*, 2060.
(10) Halperin, A.; Alexander, S. *Macromolecules* **1989**, *22*, 2403.
(11) Aniansson, E. A. G.; Wall, S. N.; Almgren, M.; Hoffman, H.; Kielmann, I.; Ulbricht, W.; Zana, R.; Lang, J.; Tondre, C. *J. Phys. Chem.* **1976**, *80*, 905.
(12) Aniansson, E. A. G.; Wall, S. N. *J. Phys. Chem.* **1974**, *78*, 1024.
(13) Dormidontova, E. E. *Macromolecules* **1999**, *32*, 7630.
(14) Wang, Y.; Matiice, W. L.; Napper, D. H. *Langmuir* **1993**, *9*, 66.
(15) Nyrkova, I. A.; Semenov, A. N. *Macromol. Theory Simul.* **2005**, *14*, 569.
(16) Iyama, K.; Nose, T. *Macromolecules* **1998**, *31*, 7356.
(17) Bednar, B.; Edwards, K.; Almgren, M.; Tormod, S.; Tuzar, Z. *Makromol. Chem., Rapid Commun.* **1988**, *9*, 785.
(18) Zhang, Y.; Wu, T.; Liu, S. *Macromol. Chem. Phys.* **2007**, *208*, 2492.
(19) Michels, B.; Waton, G.; Zana, R. *Langmuir* **1997**, *13*, 3111.
(20) Willner, L.; Poppe, A.; Monkenbusch, M.; Richter, D. *Europhys. Lett.* **2001**, *55*, 667.
(21) Wilhelm, M.; Zhao, C. L.; Wang, Y. C.; Xu, R. L.; Winnik, M. A.; Mura, J. L.; Riess, G.; Croucher, M. D. *Macromolecules* **1991**, *24*, 1033.
(22) Wang, Y.; Kausch, C. M.; Chun, M.; Quirk, R. P.; Mattice, W. L. *Macromolecules* **1995**, *28*, 904.
(23) Prochazka, K.; Bednar, B.; Mukhtar, E.; Svoboda, P.; Trnena, J.; Almgren, M. *J. Phys. Chem.* **1991**, *95*, 4563.
(24) Lund, R.; Willner, L.; Richter, D.; Dormidontova, E. E. *Macromolecules* **2006**, *39*, 4566.
(25) Lund, R.; Willner, L.; Stellbrink, J.; Lindner, P.; Richter, D. *Phys. Rev. Lett.* **2006**, *96*, 068302.
(26) Lund, R.; Willner, L.; Richter, D.; Iatrou, H.; Hadjichristidis, N.; Lindner, P. *J. Appl. Crystallogr.* **2007**, *40*, s327.
(27) Choi, S. H.; Lodge, T. P.; Bates, F. S. *Phys. Rev. Lett.* **2010**. *104*, in press.
(28) Zana, R. *Dynamics of Surfactant Self-Assemblies: Micelles, Microemulsions, Vesicles, and Lyotropic Phase*; CRC Press: Boca Raton, FL, 2005.
(29) Chen, L.; Shen, H. W.; Eisenberg, A. *J. Phys. Chem. B* **1999**, *103*, 9488.
(30) Underhill, R. S.; Ding, J.; Birss, V. I.; Liu, G. *Macromolecules* **1997**, *30*, 8298.
(31) Meli, L.; Lodge, T. P. *Macromolecules* **2009**, *42*, 580.
(32) Lodge, T. P. *Science* **2008**, *321*, 50.
(33) Wilkes, J. S. *Green Chem.* **2002**, *4*, 73.
(34) Anderson, J. L.; Ding, J.; Welton, T.; Armstrong, D. W. *J. Am. Chem. Soc.* **2002**, *124*, 14247.
(35) Ueki, T.; Watanabe, M. *Macromolecules* **2008**, *41*, 3739.
(36) He, Y.; Li, Z.; Simone, P.; Lodge, T. P. *J. Am. Chem. Soc.* **2006**, *128*, 2745.
(37) Simone, P. F.; Lodge, T. P. *Macromol. Chem. Phys.* **2007**, *208*, 339.
(38) Ueki, T.; Watanabe, M.; Lodge, T. P. *Macromolecules* **2009**, *42*, 1315.
(39) Tamura, S.; Ueki, T.; Ueno, K.; Kodama, K.; Watanabe, M. *Macromolecules* **2009**, *42*, 6239.
(40) Hillmyer, M. A.; Bates, F. S. *Macromolecules* **1996**, *29*, 6994.
(41) Mao, H. Nanoporous Polymer with Functionalized 1-D and 3-D Channels from Ordered Block Copolymer Templates. Ph.D. Thesis University of Minnesota, **2006**; p 78.
(42) Simone, P. M.; Lodge, T. P. *Macromolecules* **2008**, *41*, 1753.
(43) Brown, W. *Dynamic Light Scattering: The Method and Some Applications*; Oxford University Press: New York, 1993.
(44) Bai, Z.; He, Y.; Lodge, T. P. *Langmuir* **2008**, *24*, 5284.
(45) Tokuda, H.; Hayamizu, K.; Ishii, K.; Hasan Susan, A. B.; Watanabe, M. *J. Phys. Chem. B* **2004**, *108*, 16593.
(46) Jakes, J. *Collect. Czech. Chem. Commun.* **1995**, *60*, 1781.
(47) Webber, S. E.; Munk, P.; Tuzar, Z. *Solvents and Self-Organization of Polymers*; NATO Science Series E; 1996, Vol. *327*.
(48) Moldovan, P. L.; Strazielle, C. *Makromol. Chem.* **1970**, *140*, 201.
(49) Zhang, L.; Eisenberg, A. *Macromolecules* **1999**, *32*, 2239.
(50) Lee, S. H.; Lee, S. B. *Chem. Commun.* **2005**, 3469.
(51) Brandrup, J.; Immergut, E. H.; Grulke, E. A. *Polymer Handbook*; Wiley-Interscience: New York, 1999.
(52) Xu, R.; Winnik, A.; Hallett, F. R.; Riess, G.; Croucher, M. D. *Macromolecules* **1991**, *24*, 87.
(53) Bronstein, L. M.; Chernyshov, D. M.; Timofeeva, G. I.; Dubrovina, L. V.; Valetsky, P. M.; Khokhlov, A. R. *Langmuir* **1999**, *15*, 6195.
(54) Ruegg, M. L.; Patel, A. J.; Narayanan, S.; Sandy, A. R.; Mochrie, S. G. J.; Watanabe, H.; Balsara, N. P. *Macromolecules* **2006**, *39*, 8822.
(55) Dalvi, M. C.; Lodge, T. P. *Macromolecules* **1993**, *26*, 859.
(56) Yokoyama, H.; Kramer, E. J. *Macromolecules* **1998**, *31*, 7871.
(57) Cavicchi, K. A.; Lodge, T. P. *Macromolecules* **2003**, *36*, 7158.
(58) Fredrickson, G. H.; Milner, S. T. *Mater. Res. Soc. Symp. Proc.* **1990**, *117*, 169.
(59) Won, Y. Y.; Brannan, A. K.; Davis, H. T.; Bates, F. S. *J. Phys. Chem. B* **2002**, *106*, 3354.
(60) Zhang, J.; Xu, J.; Liu, S. *J. Phys. Chem. B* **2008**, *112*, 11284.
(61) Won, Y. Y.; Davis, H. T.; Bates, F. S. *Macromolecules* **2003**, *36*, 953.